

# Magnetic-field tuning of photo-induced superconductivity in striped $\text{La}_{2-x}\text{Ba}_x\text{CuO}_4$

D. Nicoletti<sup>1,\*</sup>, D. Fu<sup>1</sup>, O. Mehio<sup>1</sup>, S. Moore<sup>1</sup>, A. S. Disa<sup>1</sup>, G. D. Gu<sup>2</sup>, and A. Cavalleri<sup>1,3</sup>

<sup>1</sup> Max Planck Institute for the Structure and Dynamics of Matter, Hamburg, Germany

<sup>2</sup> Condensed Matter Physics and Materials Science Department,  
Brookhaven National Laboratory, Upton, NY, United States

<sup>3</sup> Department of Physics, Clarendon Laboratory, University of Oxford, Oxford, United Kingdom

\* e-mail: daniele.nicoletti@mpsd.mpg.de

## Abstract

*Optical excitation of stripe-ordered  $\text{La}_{2-x}\text{Ba}_x\text{CuO}_4$  has been shown to transiently enhance superconducting tunneling between the  $\text{CuO}_2$  planes. This effect was revealed by a blue-shift, or by the appearance of a Josephson Plasma Resonance in the terahertz-frequency optical properties. Here, we show that this photo-induced state can be strengthened by the application of high external magnetic fields oriented along the  $c$ -axis. For a 7-Tesla field, we observe up to a ten-fold enhancement in the transient interlayer phase correlation length, accompanied by a two-fold increase in the relaxation time of the photo-induced state. These observations are highly surprising, since static magnetic fields suppress interlayer Josephson tunneling and stabilize stripe order at equilibrium. We interpret our data as an indication that optically-enhanced interlayer coupling in  $\text{La}_{2-x}\text{Ba}_x\text{CuO}_4$  does not originate from a strengthening of the equilibrium superconductor that competes with stripes, as previously hypothesized. Rather, these results suggest that the photo-induced state may emerge from activated tunneling between optically-excited pair-density-waves in adjacent planes.*

Charge and spin ordered phases are found throughout wide regions of the phase diagrams of high- $T_c$  cuprates<sup>1,2,3,4,5,6,7</sup>. These orders tend to compete with the superconducting state, reducing its coherence. A well-studied case is that of single-layer compounds, in which the doped holes arrange themselves in one-dimensional charge stripes separated by regions of oppositely phased antiferromagnetic order in the  $\text{CuO}_2$  planes. In  $\text{La}_{2-x}\text{Ba}_x\text{CuO}_4$  (LBCO), for example, stripes completely suppress superconductivity at  $x = 1/8$  doping<sup>8,9</sup>, and coexist with it at lower and higher doping values (see phase diagram in Fig. 1(a)).

Stripe order in LBCO is generally stabilized by a low-temperature tetragonal (LTT) phase<sup>10,11</sup>, a structural phase in which the fourfold rotational symmetry of the  $\text{CuO}_2$  planes is broken by the buckling of the oxygen octahedra which alternates between adjacent planes<sup>12</sup>. However, stripes have also been observed without any LTT distortion<sup>13,14</sup>, indicating that charge ordering may in fact be driven purely by electronic phenomena. Recent experimental evidence<sup>15,16</sup> suggests that the individual striped planes may be made up of a spatially modulated superfluid, a so-called “pair-density-wave” (PDW), in which the interlayer Josephson tunneling is frustrated by symmetry (see  $90^\circ$  stacking in inset of Fig. 1(a))<sup>17,18</sup>. The presence of such PDW state in these compounds, extending up to the charge ordering temperature  $T_{\text{CO}}$ , was also recently verified by means of nonlinear THz spectroscopy<sup>19</sup>.

Pressure and magnetic fields have been used to tune the striped state in LBCO and in related compounds. In particular, hydrostatic pressures of few GPa were shown to increase  $T_c$  (Ref. 20), to symmetrize the crystal lattice by removing the LTT distortion, and to partially suppress charge order<sup>13</sup>. On the other hand, magnetic fields  $H \lesssim 10$  T (in particular those oriented in the direction perpendicular to the planes,  $H \parallel c$ ) were

shown to amplify the effect of dynamical layer decoupling, leading to a reduction of interlayer tunneling<sup>21,22</sup> and the stabilization of charge- and spin-order<sup>23,24</sup>.

More recently, optical excitation with femtosecond laser pulses has emerged as a means to drive the interplay between stripes and superconductivity<sup>25</sup>, enhancing one or the other transiently. Excitation of either the in-plane Cu-O stretching mode in non-superconducting, LTT distorted  $\text{La}_{1.675}\text{Eu}_{0.2}\text{Sr}_{0.125}\text{CuO}_4$  (LESCO<sub>1/8</sub>)<sup>26,27</sup>, or of  $\text{La}_{2-x}\text{Ba}_x\text{CuO}_4$  with high-energy (1.5 eV) optical pulses<sup>28,29</sup>, were both shown to enhance interlayer tunneling<sup>30</sup>.

In these photo-induced superconductivity experiments, the enhancement was achieved at or near 1/8 doping levels, and it was generally interpreted as a consequence of the removal of frustration by ultrafast melting of stripes<sup>31,32</sup>.

Here, we study this effect by tuning the relative strength of equilibrium interlayer tunneling and stripes before photo-excitation. This is investigated for different doping levels, as a function of temperature, and in presence of external magnetic fields up to 7 T. The experiments yield highly surprising results and identify a correlation between the strength of the equilibrium stripe phase (before it is optically melted) and the photo-induced superconducting state. Contrary to what is expected, we find that the presence of a strong equilibrium interlayer coupling is detrimental and not beneficial to the strength of the photo-induced state.

The  $\text{La}_{2-x}\text{Ba}_x\text{CuO}_4$  single crystals used in our experiments were grown at two nominal Ba concentrations  $x = 9.5\%$  and  $11.5\%$ <sup>33</sup>. Both of these compounds are superconducting, with transitions at  $T_C \simeq 32$  and  $13$  K, respectively. At 9.5% doping, charge- and spin-order, the structural transition and superconductivity all appear at the same temperature  $T_{CO} \simeq T_{SO} \simeq T_{LT} \simeq T_C \simeq 32$  K, while these transitions become

decoupled at higher hole concentrations ( $T_{CO} \approx T_{LT} \approx 53$  K and  $T_{SO} \approx 40$  K for  $x = 11.5\%$ , see phase diagram in Fig. 1(a)).

All measurements were carried out in a superconducting magnet with optical access, with magnetic fields up to 7 T applied along the direction perpendicular to the  $\text{CuO}_2$  planes (parallel to the  $c$  axis), and for temperatures down to  $\sim 5$  K (see Fig. 1(b) for experimental geometry).

The equilibrium optical properties<sup>34</sup> at both doping levels were determined using single-cycle THz pulses polarized along the  $c$  axis (see Fig. 1(b)), whose electric field profile was measured after reflection from the sample surface at different temperatures, both below and above  $T_c$ <sup>35</sup>. The  $c$ -axis equilibrium reflectivities extracted with this procedure are shown in the left-hand panel of Fig. 1(c) for  $H = 0$  and  $T = 5$  K. Both spectra are characterized by a Josephson Plasma Resonance (JPR), which appears at  $\sim 0.5$  THz for  $x = 9.5\%$  and at  $\sim 0.2$  THz for  $x = 11.5\%$ .

In the time resolved experiments, the LBCO crystals were photo-excited with  $\sim 100$  fs, 800 nm wavelength laser pulses, also polarized along the  $c$  axis (see Fig. 1(b)), at a fluence of  $\sim 2$  mJ/cm<sup>2</sup>. The pump photon energy is indicated by arrows in the equilibrium reflectivity and optical conductivity spectra (Fig. 1(c)). Changes in the real and imaginary  $c$ -axis optical properties were retrieved for different time delays after photo-excitation with a temporal resolution of  $\sim 300$  fs<sup>36</sup>, having taken into account the pump-probe penetration depth mismatch<sup>37</sup>.

The optical response of the 11.5%-doped compound ( $T < T_c$ ), measured in absence of magnetic field, is displayed in Fig. 2(a-d), both at equilibrium (gray) and at two different pump-probe time delays ( $\tau = 1.4$  ps and  $\tau = 2$  ps) after photo-excitation (blue circles). As already reported in Refs. 28,29 this material was found to be the most photo-

susceptible within the LBCO family, displaying optically-enhanced (induced) superconductivity all the way up to  $T_{S0} \simeq 40$  K.

The  $\tau = 1.4$  ps data show a strong optically-induced increase in superfluid stiffness, evidenced by a blue-shift of the JPR from  $\sim 0.2$  THz to  $\sim 0.6$  THz (reflectivity edge in Fig. 2(a)), and, correspondingly, by an enhancement in the low-frequency imaginary conductivity  $\sigma_2(\omega)$  (Fig. 2(c))<sup>38</sup>. The data shown in Fig. 2(a) and Fig. 2(c) could be fitted using a model that describes the optical response of a Josephson plasma, for which the dielectric function is expressed as  $\tilde{\epsilon}(\omega) = \epsilon_\infty(1 - \omega_J^2/\omega^2)$ . Fits to the transient spectra are displayed as blue lines<sup>39</sup>.

At longer time delay ( $\tau = 2$  ps), the response was observed to evolve into that of a conductor with finite carrier scattering rate, as evidenced by the broadening of the reflectivity edge (Fig 2(b)) and by the appearance of a peak at finite frequency in  $\sigma_2(\omega)$  (Fig. 2(d))<sup>38</sup>. Notably, the response functions at this longer time delay could be fitted using a conventional Drude model for metals (blue lines in Fig. 2(b) and Fig. 2(d)), for which the complex dielectric function is expressed as  $\tilde{\epsilon}(\omega) = \epsilon_\infty[1 - \omega_p^2/(\omega^2 + i\Gamma\omega)]$ . Here,  $\omega_p$  and  $\Gamma$  are the carrier plasma frequency and scattering rate, respectively.

The same experiment was repeated in a 7 T magnetic field, oriented along the  $c$  axis. At equilibrium, the application of the magnetic field induces vortices within the  $\text{CuO}_2$  layers, stabilizes charge and spin order<sup>24</sup>, and suppresses interlayer Josephson coupling<sup>21</sup> without appreciably affecting superconductivity in the planes (as  $H_{c2} \gg 7$  T). The magnetic-field-induced suppression of interlayer superfluid stiffness is evidenced by the red-shifted equilibrium JPR, which for zero field is found at  $\sim 0.2$  THz (gray line in Fig. 2(a)), while in a 7 T magnetic field it is quenched to below the probed frequency range ( $< 0.1$  THz, gray line in Fig. 2(e)).

Similar to the data of Fig. 2(a), also in this case a clear edge appeared in the transient reflectivity measured 1.4 ps after photo-excitation (Fig. 2(e), red circles). However, in this in-field measurement, the transient JPR remained sharp for longer time delays (Fig. 2(f)), revealing superconducting-like optical properties even at  $\tau = 2$  ps. This is also evidenced by the diverging  $\sigma_2(\omega \rightarrow 0)$  in Fig. 2(h)<sup>38</sup>. Remarkably, unlike the zero-field data in Fig. 2(a-d), the transient optical properties measured at 7 T could be fitted with the Josephson plasma formula at both time delays shown in Fig. 2(e-h).

The coherent character of this newly discovered optically-induced superconducting state in presence of high magnetic fields is even more evident in Fig. 3. Here, we show, for different data sets, the dynamical evolution of the interlayer phase correlation length, extracted from the Drude fits of Fig. 2 and defined as  $\xi_c = 2\omega_p L/\Gamma$  (here  $L$  is the CuO<sub>2</sub> layer separation)<sup>27</sup>. Note that at the earliest time delays, for which the optical properties could also be fitted with a JPR model,  $\xi_c$  is at least  $\sim 20$  unit cells. The upper bound is here determined by the frequency resolution of our measurement. At longer delays instead, for which the response is well described by the Drude model,  $\xi_c$  becomes finite and exhibits a collapse, within a few picoseconds, down to values close to 1-2 unit cells. This collapse became slower and not faster when the temperature was raised to 30 K (Fig. 3(a)), and it was observed to be even slower in presence of a 7 T magnetic field (Fig. 3(b)). Notably, the application of magnetic field resulted, for certain time delays ( $\tau \simeq 1-2$  ps) in a  $\sim 10$ -fold increase in  $\xi_c$ .

An additional piece of information is added here by the measurements performed at  $T_c < T < T_{so}$  (Fig. 3(a))<sup>38</sup>. In this case, transient superconductivity emerged from the equilibrium normal state, displaying a larger  $\xi_c$  than that found at lower temperatures. This observation suggests that, for  $H = 0$ , the transient superconductor induced from

the normal state is “more coherent” than that induced by exciting the superconducting state at  $T < T_c$ .

Importantly, all data reported in Fig. 3 display relaxation dynamics to a state with only partially reduced coherence. At  $\tau \gtrsim 2$  ps, the data could still be fitted with carrier scattering rates of  $\Gamma \simeq 1$  THz (corresponding to  $\xi_c \sim 1-2$  unit cells, see also Ref. 28), values that are anomalously low for conventional incoherent charge transport, and are rather suggestive of a strongly fluctuating superconducting state<sup>40</sup>.

The full dynamical response, determined for a wide variety of initial conditions (different doping values, temperatures, external magnetic fields) is shown in Fig. 4. Here, we plot the frequency- and time-delay-dependent energy loss function,  $\Im[-1/\tilde{\epsilon}(\omega, \tau)]$ , as extracted from fits to the transient optical response functions. This quantity exhibits a sharp peak at the JPR frequency, which acquires a finite width  $\Gamma$  as soon as scattering processes set in.

Figure 4(a) displays the response of the 9.5%-doped compound<sup>38</sup> below  $T_c$  at zero field, that was already reported in Ref. 28. This material, for which the equilibrium superconducting phase is robust (see equilibrium JPR at  $\sim 0.5$  THz) and stripe order is weak<sup>9</sup>, only shows marginal superconductivity enhancement for  $\tau \lesssim 1$  ps, and then, at later delays, it evolves abruptly into an incoherent state, characterized by an overdamped loss function peak. As reported in Ref. 28,  $\text{La}_{1.905}\text{Ba}_{0.095}\text{CuO}_4$  shows no light-induced response for  $T > T_c \simeq T_{CO} \simeq T_{SO}$ .

When a 7 T magnetic field is applied to the 9.5% compound (Fig. 4(b)), the equilibrium interlayer superfluid stiffness is reduced with respect to that measured at zero field (the JPR at  $\tau \leq 0$  ps is now at  $\sim 0.2$  THz) and, concomitantly, stripe order is enhanced by  $\sim 30\%$ <sup>24</sup>. Here, the optically-induced effect was different from that measured in the same material at  $H = 0$  and resembled that found at 11.5% doping. Within  $\sim 1.5$  ps after

photo-excitation, a notable blue-shift of the equilibrium JPR developed, reaching values close to 0.5 THz<sup>38</sup>. This observation suggests that interlayer Josephson tunneling, which was almost completely quenched by the magnetic field, can be transiently revived also at 9.5% doping by photo-excitation. However, this revival occurs only over a short time interval, and for  $\tau \gtrsim 1.5$  ps the system evolves abruptly into an incoherent state, characterized by an overdamped loss function, similar to that found at long delays for  $H = 0$  (Fig. 4(a)).

The middle and lower panels of Fig. 4 (panels c-f) show the  $\Im m[-1/\tilde{\epsilon}(\omega, \tau)]$  function of the 11.5% compound, for which selected optical spectra are displayed in Fig. 2 and the extracted phase correlation lengths are reported in Fig. 3<sup>38</sup>. Note that this compound is characterized by weaker equilibrium interlayer superfluid stiffness and by a far stronger stripe order than that found at 9.5% doping (by a factor of  $\sim 5$ )<sup>9</sup>.

The dynamical evolution of the loss function in this compound displays, for all temperatures and applied magnetic field values, a more “coherent” character than that found in  $\text{La}_{1.905}\text{Ba}_{0.095}\text{CuO}_4$  (Fig. 4(a-b)). In particular, the data taken at  $T = 5$  K and  $H = 7$  T (Fig. 4(f)) are those showing the sharper JPR, with the longer lifetime.

All the results above clearly indicate that optically-enhanced (induced) superconductivity in  $\text{La}_{2-x}\text{Ba}_x\text{CuO}_4$  correlates with the strength of the equilibrium stripe order. Indeed, the stronger the stripes, the longer the photo-induced coherence, as shown by systematically changing the doping level, sample temperature and external magnetic field. An exception to this trend is found in the temperature dependent response of LBCO 11.5% (Fig. 3(a) and Fig. 4(c-d)). Here, the transient lifetime is clearly enhanced in the 30 K data, although the equilibrium charge order is reduced by  $\sim 15\%$  with respect to lower temperatures<sup>9</sup>.



The observations above can be interpreted by considering the role of the equilibrium, pre-existing *c*-axis superfluid stiffness in determining the properties of the transient state. Our data suggest that a more robust superconductor at equilibrium adversely affects the strength and lifetime of transient Josephson coupling (see Fig. 4(a)), while a weak or completely absent pre-existing condensate (Fig. 4(d-f)) promotes the transient superconducting state.

The equilibrium and optically-induced interlayer tunneling might indeed originate from two separate entities. The former is a spatially homogeneous in-plane condensate, which contributes to the interlayer superfluid stiffness at equilibrium, and whose density is higher for dopings away from 1/8 (as in LBCO 9.5%). The latter, within a PDW picture<sup>18</sup>, may be understood as originating from superconducting stripes, whose Josephson tunneling is activated via photo-excitation and whose strength, as for the stripes, is maximum close to 1/8 doping. The equilibrium superconductor and the photo-excited PDW may well compete rather than cooperate with each other, similar to how static charge- and spin-order compete with 3D superconductivity at equilibrium.

In the aggregate, the results reported above set new constraints on the overall origin of light-induced superconductivity in single-layer cuprates, which appears to result from the photo-excited striped phase and perhaps is not easily explained as simple optical melting of stripes<sup>31</sup>.

## **Acknowledgments**

The research leading to these results received funding from the European Research Council under the European Union's Seventh Framework Programme (FP7/2007-2013)/ERC Grant Agreement No. 319286 (QMAC). We acknowledge support from the Deutsche Forschungsgemeinschaft via the excellence cluster 'The Hamburg Centre for Ultrafast Imaging—Structure, Dynamics and Control of Matter at the Atomic Scale' and the priority program SFB925. Work at Brookhaven is supported by the Office of Basic Energy Sciences, Division of Materials Sciences and Engineering, U.S. Department of Energy under Contract No. DE-SC0012704.

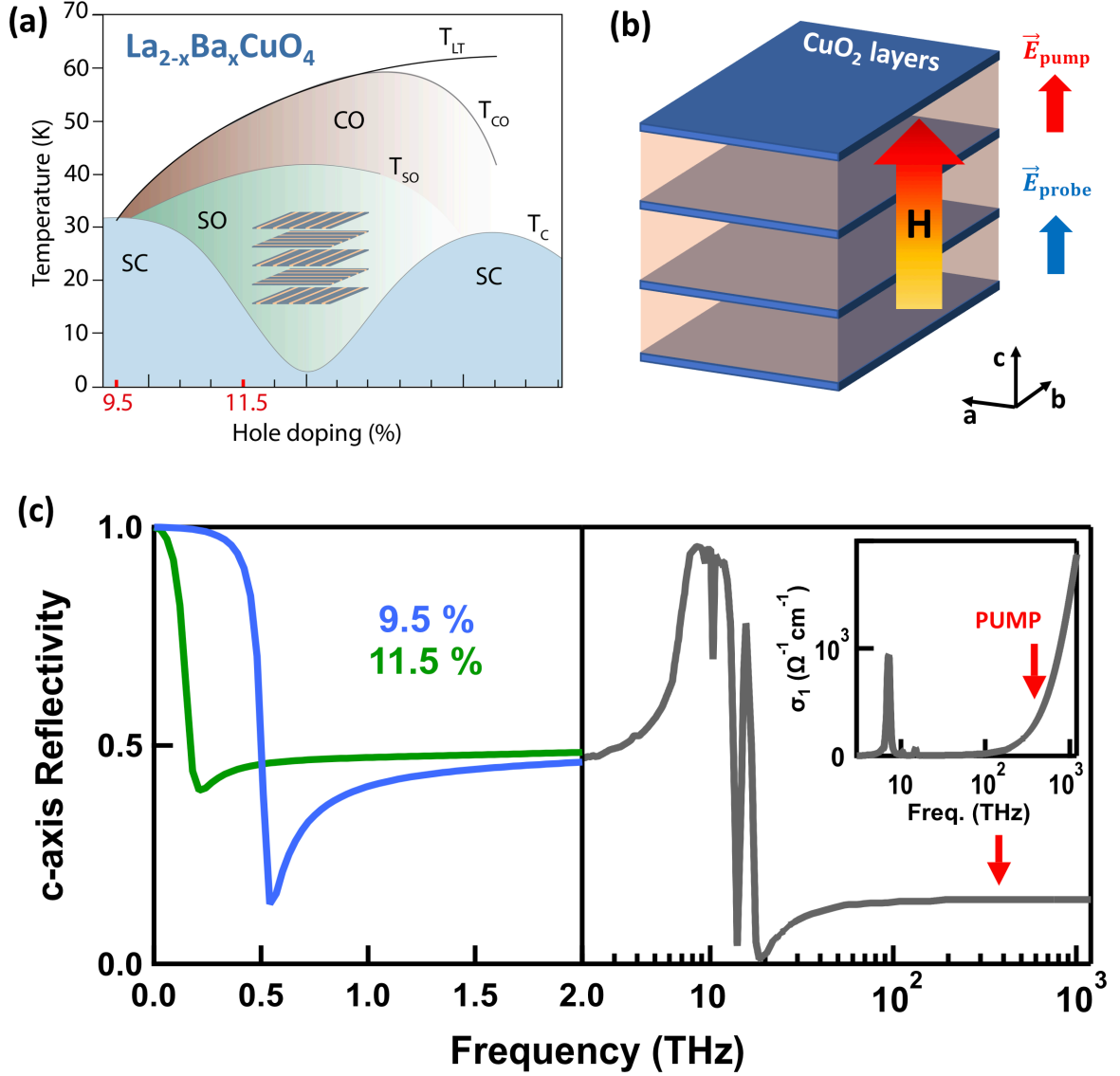


**Figure 1.** (a) Temperature-doping phase diagram of  $\text{La}_{2-x}\text{Ba}_x\text{CuO}_4$  (LBCO), as determined in Ref. 9.  $T_C$ ,  $T_{CO}$ ,  $T_{SO}$ , and  $T_{LT}$  indicate the superconducting, charge-order, spin-order, and structural transition temperatures, respectively. The dopings investigated in this experiment are highlighted in red. The inset shows the periodic stacking of  $\text{CuO}_2$  planes in the stripe phase. The stripe orientation rotates by  $90^\circ$  between layers. (b) Cartoon depicting the experimental geometry. LBCO crystals were photo-excited with optical pulses polarized along the  $c$ -axis. Delayed THz probe pulses, also polarized along  $c$ , were used to measure snapshots of the complex response functions of the perturbed material. The experiment was repeated in presence of magnetic fields up to 7 T, oriented along the  $c$  direction. (c) Equilibrium  $c$ -axis optical properties of LBCO. Left panel: THz reflectivity of both samples at  $T = 5$  K (no magnetic field). Right panel and inset: broadband  $c$ -axis reflectivity and optical conductivity of LBCO from Ref. 34. Red arrows indicate the pump photon energy.

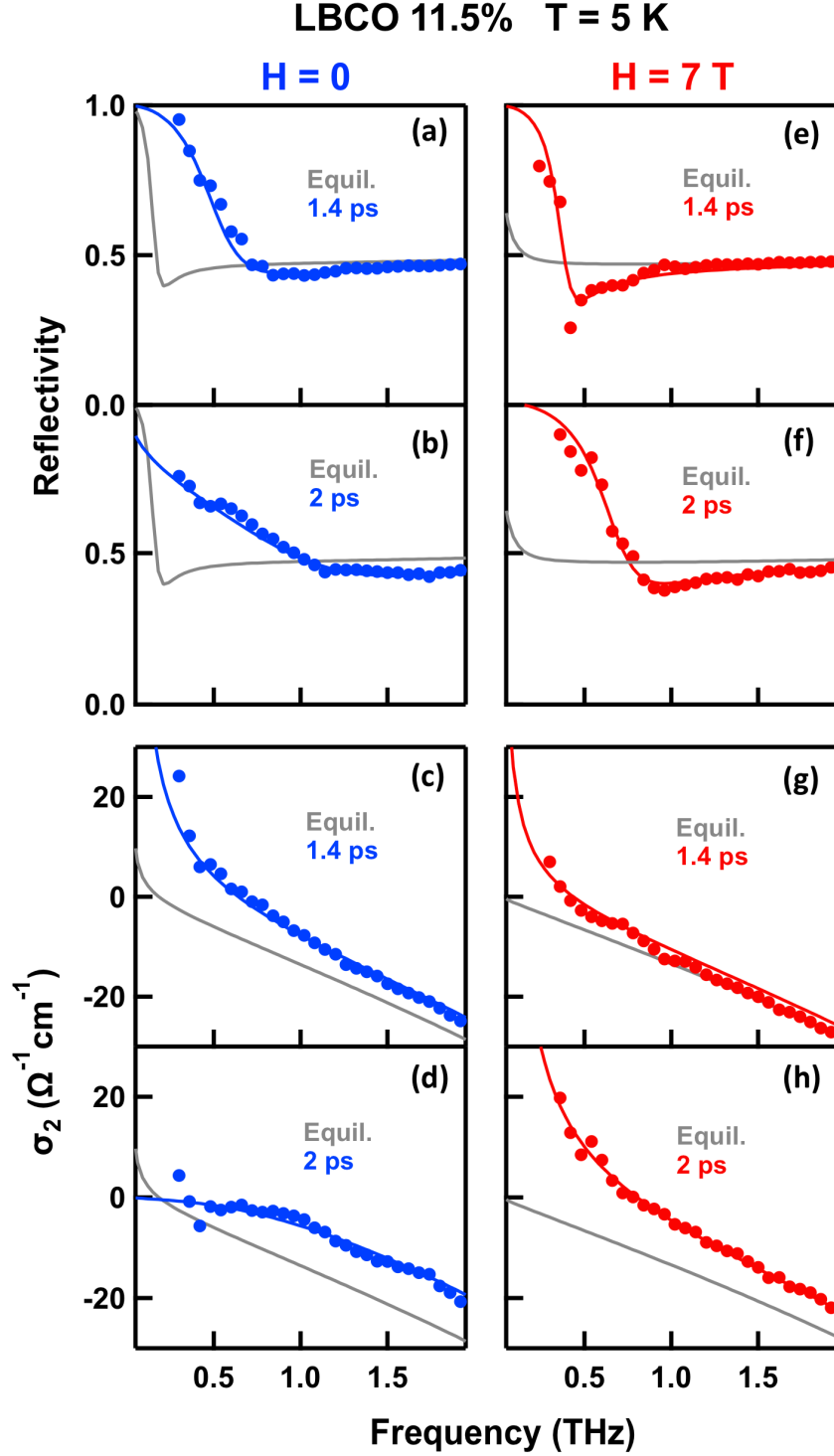


**Figure 2.** (a,b) *c*-axis THz reflectivity of  $\text{La}_{1.885}\text{Ba}_{0.115}\text{CuO}_4$  measured at  $T = 5$  K (no magnetic field), at equilibrium (gray lines) and at two pump-probe time delays ( $\tau = 1.4$  ps and  $\tau = 2$  ps) after excitation (blue circles). Fits to the transient spectra (see main text) are shown as blue lines. (e,f) Same quantities as in (a,b) measured in  $\text{La}_{1.885}\text{Ba}_{0.115}\text{CuO}_4$  at  $T = 5$  K in presence of a 7 T magnetic field (transient data are shown here in red). (c,d) Zero-field imaginary conductivity spectra corresponding to the reflectivities shown in (a,b). (g,h) In-field imaginary conductivities corresponding to the data of (e,f).

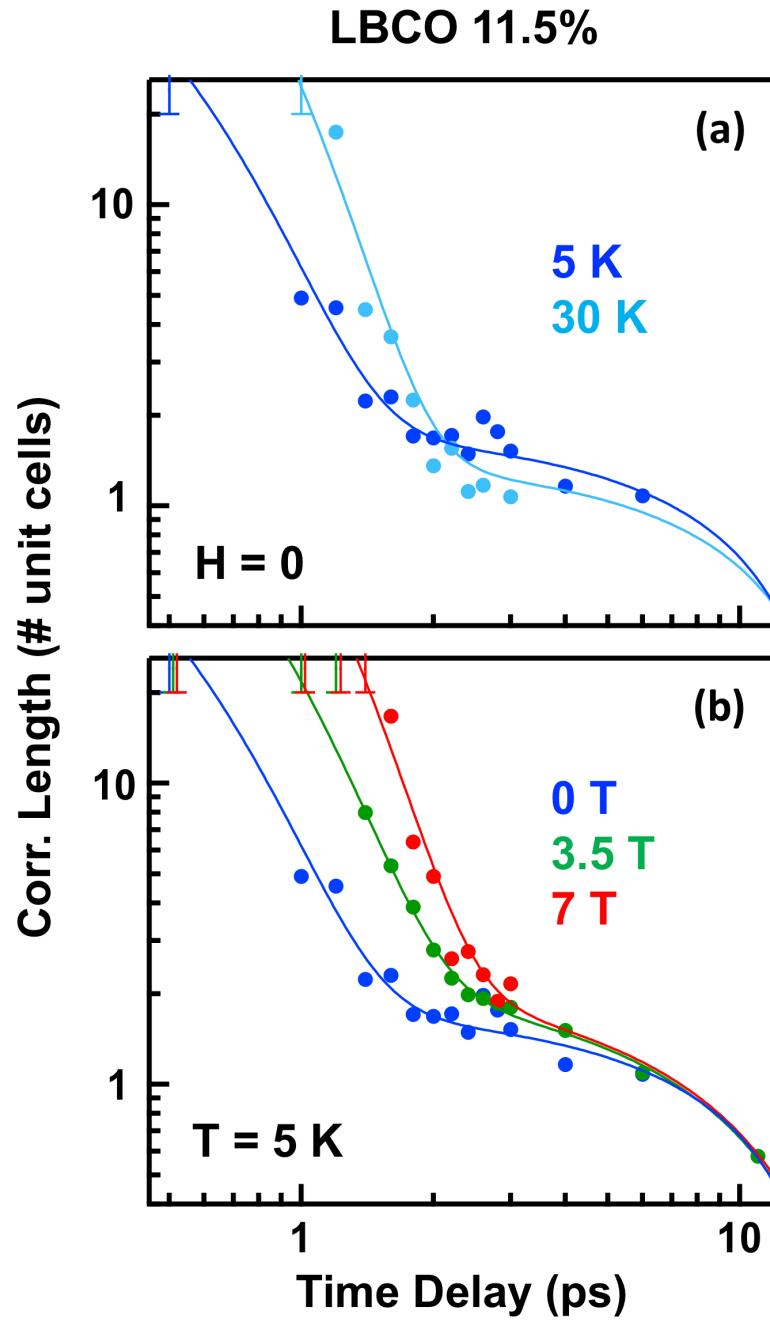


**Figure 3.** Dynamical evolution of the interlayer phase correlation length measured in  $\text{La}_{1.885}\text{Ba}_{0.115}\text{CuO}_4$  for different temperatures and applied magnetic fields. The values were extracted from the fits of Fig. 2 (see main text).

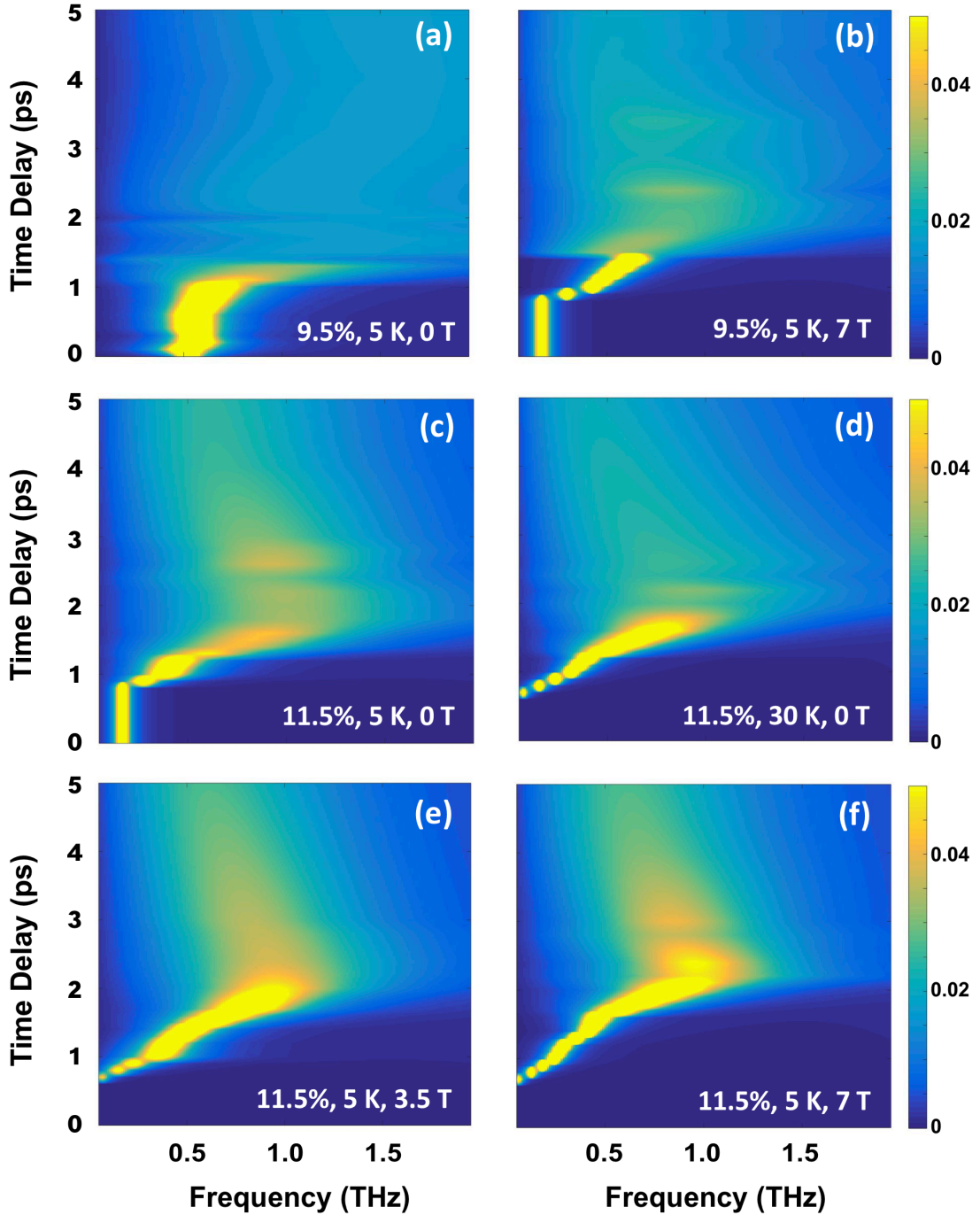


**Figure 4.** Dynamical evolution of the energy loss function of photo-stimulated LBCO under various starting conditions (different doping levels, sample temperatures, and applied magnetic field values), as extracted from fits to the data (see main text). Panels (a,b) refer to the  $\text{La}_{1.905}\text{Ba}_{0.095}\text{CuO}_4$  compound at  $T = 5$  K in absence (a) and in presence (b) of a 7 T magnetic field. Panels (c-f) show instead the response of  $\text{La}_{1.885}\text{Ba}_{0.115}\text{CuO}_4$ , measured at  $T = 5$  K and  $H = 0$  (c),  $T = 30$  K and  $H = 0$  (d),  $T = 5$  K and  $H = 3.5$  T (e),  $T = 5$  K and  $H = 7$  T (f). Panels are ordered from (a) to (f) by increasingly stronger equilibrium stripe order, with the exception of panel (d) ( $T = 30$  K data), for which charge order was measured to be weaker than at lower temperatures (panel (c), see main text).

## REFERENCES

- 
- <sup>1</sup> J. M. Tranquada, B. J. Sternlieb, J. D. Axe, Y. Nakamura, and S. Uchida, "Evidence for stripe correlations of spins and holes in copper oxide superconductors", *Nature* **375**, 561 (1995).
- <sup>2</sup> C. V. Parker, P. Aynajian, E. H. da Silva Neto, A. Pushp, S. Ono, J. Wen, Z. Xu, G. Gu, and A. Yazdani, "Fluctuating stripes at the onset of the pseudogap in the high- $T_C$  superconductor  $\text{Bi}_2\text{Sr}_2\text{CaCu}_2\text{O}_{8+x}$ ", *Nature* **468**, 677 (2010).
- <sup>3</sup> T. Wu, H. Mayaffre, S. Krämer, M. Horvatić, C. Berthier, W. N. Hardy, R. Liang, D. A. Bonn, and M.-H. Julien, "Magnetic-field-induced charge-stripe order in the high-temperature superconductor  $\text{YBa}_2\text{Cu}_3\text{O}_y$ ", *Nature* **477**, 191 (2011).
- <sup>4</sup> G. Ghiringhelli, M. Le Tacon, M. Minola, S. Blanco-Canosa, C. Mazzoli, N. B. Brookes, G. M. De Luca, A. Frano, D. G. Hawthorn, F. He, T. Loew, M. Moretti Sala, D. C. Peets, M. Salluzzo, E. Schierle, R. Sutarto, G. A. Sawatzky, E. Weschke, B. Keimer, and L. Braicovich, "Long-Range Incommensurate Charge Fluctuations in  $(\text{Y,Nd})\text{Ba}_2\text{Cu}_3\text{O}_{6+x}$ ", *Science* **337**, 821 (2012).
- <sup>5</sup> D. H. Torchinsky, F. Mahmood, A. T. Bollinger, I. Bozovic, N. Gedik, "Fluctuating charge-density waves in a cuprate superconductor", *Nat. Mater.* **12**, 387 (2013).
- <sup>6</sup> J. Chang, E. Blackburn, A. T. Holmes, N. B. Christensen, J. Larsen, J. Mesot, Ruixing Liang, D. A. Bonn, W. N. Hardy, A. Watenphul, M. v. Zimmermann, E. M. Forgan, and S. M. Hayden, "Direct observation of competition between superconductivity and charge density wave order in  $\text{YBa}_2\text{Cu}_3\text{O}_{6.67}$ ", *Nature Physics* **8**, 871 (2012).
- <sup>7</sup> R. Comin, A. Frano, M. M. Yee, Y. Yoshida, H. Eisaki, E. Schierle, E. Weschke, R. Sutarto, F. He, A. Soumyanarayanan, Yang He, M. Le Tacon, I. S. Elfimov, Jennifer E. Hoffman, G. A. Sawatzky, B. Keimer, and A. Damascelli, "Charge Order Driven by Fermi-Arc Instability in  $\text{Bi}_2\text{Sr}_{2-x}\text{La}_x\text{CuO}_{6+\delta}$ ", *Science* **343**, 390 (2014).
- <sup>8</sup> A. R. Moodenbaugh, Youwen Xu, M. Suenaga, T. J. Folkerts, and R. N. Shelton, "Superconducting properties of  $\text{La}_{2-x}\text{Ba}_x\text{CuO}_4$ ", *Phys. Rev. B* **38**, 4596 (1988).
- <sup>9</sup> M. Hücker, M. v. Zimmermann, G. D. Gu, Z. J. Xu, J. S. Wen, Guangyong Xu, H. J. Kang, A. Zheludev, and J. M. Tranquada, "Stripe order in superconducting  $\text{La}_{2-x}\text{Ba}_x\text{CuO}_4$  ( $0.095 \leq x \leq 0.155$ )", *Phys. Rev. B* **83**, 104506 (2011).
- <sup>10</sup> Takashi Suzuki and Toshizo Fujita, "Structural phase transition in  $(\text{La}_{1-x}\text{Ba}_x)_2\text{CuO}_{4-\delta}$ ", *Physica C: Superconductivity* **159**, 111 (1989).
- <sup>11</sup> M. K. Crawford, R. L. Harlow, E. M. McCarron, W. E. Farneth, J. D. Axe, H. Chou, and Q. Huang, "Lattice instabilities and the effect of copper-oxygen-sheet distortions on superconductivity in doped  $\text{La}_2\text{CuO}_4$ ", *Phys. Rev. B* **44**, 7749 (1991).

- 
- <sup>12</sup> J. M. Tranquada, J. D. Axe, N. Ichikawa, Y. Nakamura, S. Uchida, and B. Nachumi, “Neutron-scattering study of stripe-phase order of holes and spins in  $\text{La}_{1.48}\text{Nd}_{0.4}\text{Sr}_{0.12}\text{CuO}_4$ ”, *Phys. Rev. B* **54**, 7489 (1996).
- <sup>13</sup> M. Hücker, M. v. Zimmermann, M. Debessai, J. S. Schilling, J. M. Tranquada, and G. D. Gu, “Spontaneous Symmetry Breaking by Charge Stripes in the High Pressure Phase of Superconducting  $\text{La}_{1.875}\text{Ba}_{0.125}\text{CuO}_4$ ”, *Phys. Rev. Lett.* **104**, 057004 (2010).
- <sup>14</sup> V. Thampy, M. P. M. Dean, N. B. Christensen, L. Steinke, Z. Islam, M. Oda, M. Ido, N. Momono, S. B. Wilkins, and J. P. Hill, “Rotated stripe order and its competition with superconductivity in  $\text{La}_{1.88}\text{Sr}_{0.12}\text{CuO}_4$ ”, *Phys. Rev. B* **90**, 100510(R) (2014).
- <sup>15</sup> Q. Li, M. Hücker, G. D. Gu, A. M. Tsvelik, and J. M. Tranquada, “Two-Dimensional Superconducting Fluctuations in Stripe-Ordered  $\text{La}_{1.875}\text{Ba}_{0.125}\text{CuO}_4$ ”, *Phys. Rev. Lett.* **99**, 067001 (2007).
- <sup>16</sup> M. H. Hamidian, S. D. Edkins, Sang Hyun Joo, A. Kostin, H. Eisaki, S. Uchida, M. J. Lawler, E.-A. Kim, A. P. Mackenzie, K. Fujita, Jinho Lee, and J. C. Séamus Davis, “Detection of a Cooper-pair density wave in  $\text{Bi}_2\text{Sr}_2\text{CaCu}_2\text{O}_{8+x}$ ”, *Nature* **532**, 343-347 (2016).
- <sup>17</sup> E. Berg, E. Fradkin, E.-A. Kim, S. A. Kivelson, V. Oganesyan, J. M. Tranquada, and S. C. Zhang, “Dynamical Layer Decoupling in a Stripe-Ordered High- $T_c$  Superconductor”, *Phys. Rev. Lett.* **99**, 127003 (2007).
- <sup>18</sup> E. Berg, E. Fradkin, S. A. Kivelson, and J. M. Tranquada, “Striped superconductors: how spin, charge and superconducting orders intertwine in the cuprates”, *New Journal of Physics* **11**, 115004 (2009).
- <sup>19</sup> S. Rajasekaran, J. Okamoto, L. Mathey, M. Fechner, V. Thampy, G.D. Gu, and A. Cavalleri, “Probing optically silent superfluid stripes in cuprates”, *Science* **369**, 575-579 (2018).
- <sup>20</sup> M. Ido, T. Kudo, N. Yamada, N. Momono, N. Abe, T. Nakano, C. Manabe, and M. Oda, “Pressure effect on anomalous suppression of  $T_c$  around  $x = 1/8$  in  $\text{La}_{2-x}\text{Ba}_x\text{CuO}_4$  and  $\text{La}_{1.8-x}\text{Nd}_{0.2}\text{Ba}_x\text{CuO}_4$ ”, *Journal of Low Temperature Physics* **105**, 311 (1996).
- <sup>21</sup> Z. Stegen, Su Jung Han, Jie Wu, A. K. Pramanik, M. Hücker, Genda Gu, Qiang Li, J. H. Park, G. S. Boebinger, and J. M. Tranquada, “Evolution of superconducting correlations within magnetic-field-decoupled  $\text{La}_{2-x}\text{Ba}_x\text{CuO}_4$  ( $x = 0.095$ )”, *Phys. Rev. B* **87**, 064509 (2013).
- <sup>22</sup> A. A. Schafgans, A. D. LaForge, S.V. Dordevic, M. M. Qazilbash, W. J. Padilla, K. S. Burch, Z. Q. Li, Seiki Komiya, Yoichi Ando, and D. N. Basov, “Towards a Two-Dimensional Superconducting State of  $\text{La}_{2-x}\text{Sr}_x\text{CuO}_4$  in a Moderate External Magnetic Field”, *Phys. Rev. Lett.* **104**, 157002 (2010).
- <sup>23</sup> Jungho Kim, A. Kagedan, G. D. Gu, C. S. Nelson, and Young-June Kim, “Magnetic field dependence of charge stripe order in  $\text{La}_{2-x}\text{Ba}_x\text{CuO}_4$  ( $x \approx 1/8$ )”, *Phys. Rev. B* **77**, 180513(R) (2008).

- 
- <sup>24</sup> M. Hücker, M. v. Zimmermann, Z. J. Xu, J. S. Wen, G. D. Gu, and J. M. Tranquada, “Enhanced charge stripe order of superconducting  $\text{La}_{2-x}\text{Ba}_x\text{CuO}_4$  in a magnetic field”, *Phys. Rev. B* **87**, 014501 (2013).
- <sup>25</sup> D. Nicoletti and A. Cavalleri, “Nonlinear light–matter interaction at terahertz frequencies”, *Adv. Opt. Photon.* **8**, 401-464 (2016).
- <sup>26</sup> D. Fausti, R. I. Tobey, N. Dean, S. Kaiser, A. Dienst, M. C. Hoffmann, S. Pyon, T. Takayama, H. Takagi, and A. Cavalleri, “Light-Induced Superconductivity in a Stripe-Ordered Cuprate”, *Science* **331**, 189 (2011).
- <sup>27</sup> C. R. Hunt, D. Nicoletti, S. Kaiser, T. Takayama, H. Takagi, and A. Cavalleri, “Two distinct kinetic regimes for the relaxation of light-induced superconductivity in  $\text{La}_{1.675}\text{Eu}_{0.25}\text{F}_{0.125}\text{CuO}_4$ ”, *Phys. Rev. B* **91**, 020505(R) (2015).
- <sup>28</sup> D. Nicoletti, E. Casandruc, Y. Laplace, V. Khanna, C. R. Hunt, S. Kaiser, S. S. Dhesi, G. D. Gu, J. P. Hill, A. Cavalleri, “Optically-induced superconductivity in striped  $\text{La}_{2-x}\text{Ba}_x\text{CuO}_4$  by polarization-selective excitation in the near infrared”, *Phys. Rev. B* **90**, 100503(R) (2014).
- <sup>29</sup> E. Casandruc, D. Nicoletti, S. Rajasekaran, Y. Laplace, V. Khanna, G. D. Gu, J. P. Hill, and A. Cavalleri, “Wavelength-dependent optical enhancement of superconducting interlayer coupling in  $\text{La}_{1.885}\text{Ba}_{0.115}\text{CuO}_4$ ”, *Phys. Rev. B* **91**, 174502 (2015).
- <sup>30</sup> See also: S. J. Zhang, Z. X. Wang, L. Y. Shi, T. Lin, M. Y. Zhang, G. D. Gu, T. Dong, and N. L. Wang, “Light-induced new collective modes in  $\text{La}_{1.905}\text{Ba}_{0.095}\text{CuO}_4$  superconductor”, *arXiv:1712.01174* (2017); K. Tomari, R. Matsunaga, H. Niwa, D. Song, H. Eisaki, and R. Shimano, “Light-induced switching to a Metastable Phase in a Layered Superconductor  $\text{La}_{2-x}\text{Sr}_x\text{CuO}_4$  ( $x=0.15$ )”, *arXiv:1712.05086* (2017).
- <sup>31</sup> M. Först, R. I. Tobey, H. Bromberger, S. B. Wilkins, V. Khanna, A. D. Caviglia, Y.-D. Chuang, W. S. Lee, W. F. Schlotter, J. J. Turner, M. P. Minitti, O. Krupin, Z. J. Xu, J. S. Wen, G. D. Gu, S. S. Dhesi, A. Cavalleri, and J. P. Hill, “Melting of Charge Stripes in Vibrationally Driven  $\text{La}_{1.875}\text{Ba}_{0.125}\text{CuO}_4$ : Assessing the Respective Roles of Electronic and Lattice Order in Frustrated Superconductors”, *Phys. Rev. Lett.* **112**, 157002 (2014).
- <sup>32</sup> V. Khanna, R. Mankowsky, M. Petrich, H. Bromberger, S. A. Cavill, E. Möhr-Vorobeva, D. Nicoletti, Y. Laplace, G. D. Gu, J. P. Hill, M. Först, A. Cavalleri and S. S. Dhesi, “Restoring interlayer Josephson coupling in  $\text{La}_{1.885}\text{Ba}_{0.115}\text{CuO}_4$  by charge transfer melting of stripe order”, *Phys. Rev. B* **93**, 224522 (2016).
- <sup>33</sup> The crystals were cut and polished to give an *ac* surface of  $\sim 3$  mm diameter. For more details on the sample preparation, see Ref. 9.
- <sup>34</sup> C. C. Homes, M. Hücker, Q. Li, Z. J. Xu, J. S. Wen, G. D. Gu, and J. M. Tranquada, “Determination of the optical properties of  $\text{La}_{2-x}\text{Ba}_x\text{CuO}_4$  for several dopings, including the anomalous  $x = 1/8$  phase”, *Phys. Rev. B* **85**, 134510 (2012).
- <sup>35</sup> The THz-frequency (0.15-3 THz) reflectivity ratios measured here with time-domain spectroscopy in both samples at different temperatures (both below and above  $T_c$ ) were



---

combined with the broadband reflectivities reported in Ref. 34. By applying Kramers-Kronig transformations, a full set of equilibrium optical properties (*i.e.* complex dielectric function, complex optical conductivity, complex refractive index) could be determined at all temperatures, dopings, and magnetic fields investigated in the present experiment.

<sup>36</sup> James T. Kindt and Charles A. Schmuttenmaer, “Theory for determination of the low-frequency time-dependent response function in liquids using time-resolved terahertz pulse spectroscopy”, *Journal of Chemical Physics* **110**, 8589 (1999).

<sup>37</sup> The pump-induced changes in the amplitude and phase of the reflected THz electric field were measured at different pump-probe delays. These “raw” reflectivity changes were only ~1% due to the pump-probe penetration depth mismatch. At THz frequencies, the probe interrogates a volume that is between  $10^2$  and  $10^3$  times larger than the transformed region beneath the surface, with this mismatch being a function of frequency. Such mismatch was taken into account by modeling the response of the system as that of a homogeneously photo-excited thin layer on top of an unperturbed bulk (which retains the optical properties of the sample at equilibrium). By calculating the coupled Fresnel equations of such multi-layer system [M. Dressel and G. Grüner, *Electrodynamics of Solids*, Cambridge University Press, Cambridge (2002)], the transient optical response (reflectivity, energy loss function, complex optical conductivity) of the photo-excited layer could be derived.

<sup>38</sup> See Supplemental Material for extended data sets.

<sup>39</sup> For each given pump-probe time delay, all transient optical response functions could be simultaneously fitted by a single set of parameters. In order to reproduce the background in the optical spectra, mainly caused by phonon absorptions (see Fig. 1(c)), high-frequency Lorentz oscillators have been added, chosen for the equilibrium compound and kept constant in all fits. In the fits with the Josephson plasma formula, a small overdamped Drude term was also added to account for quasi-particle currents.

<sup>40</sup> L. S. Bilbro, R. Valdés Aguilar, G. Logvenov, O. Pelleg, I. Bozovic, and N. P. Armitage, “Temporal correlations of superconductivity above the transition temperature in  $\text{La}_{2-x}\text{Sr}_x\text{CuO}_4$  probed by terahertz spectroscopy”, *Nature Physics* **7**, 298 (2011).

# SUPPLEMENTAL MATERIAL

LBCO 11.5%  $T = 5$  K  $H = 0$

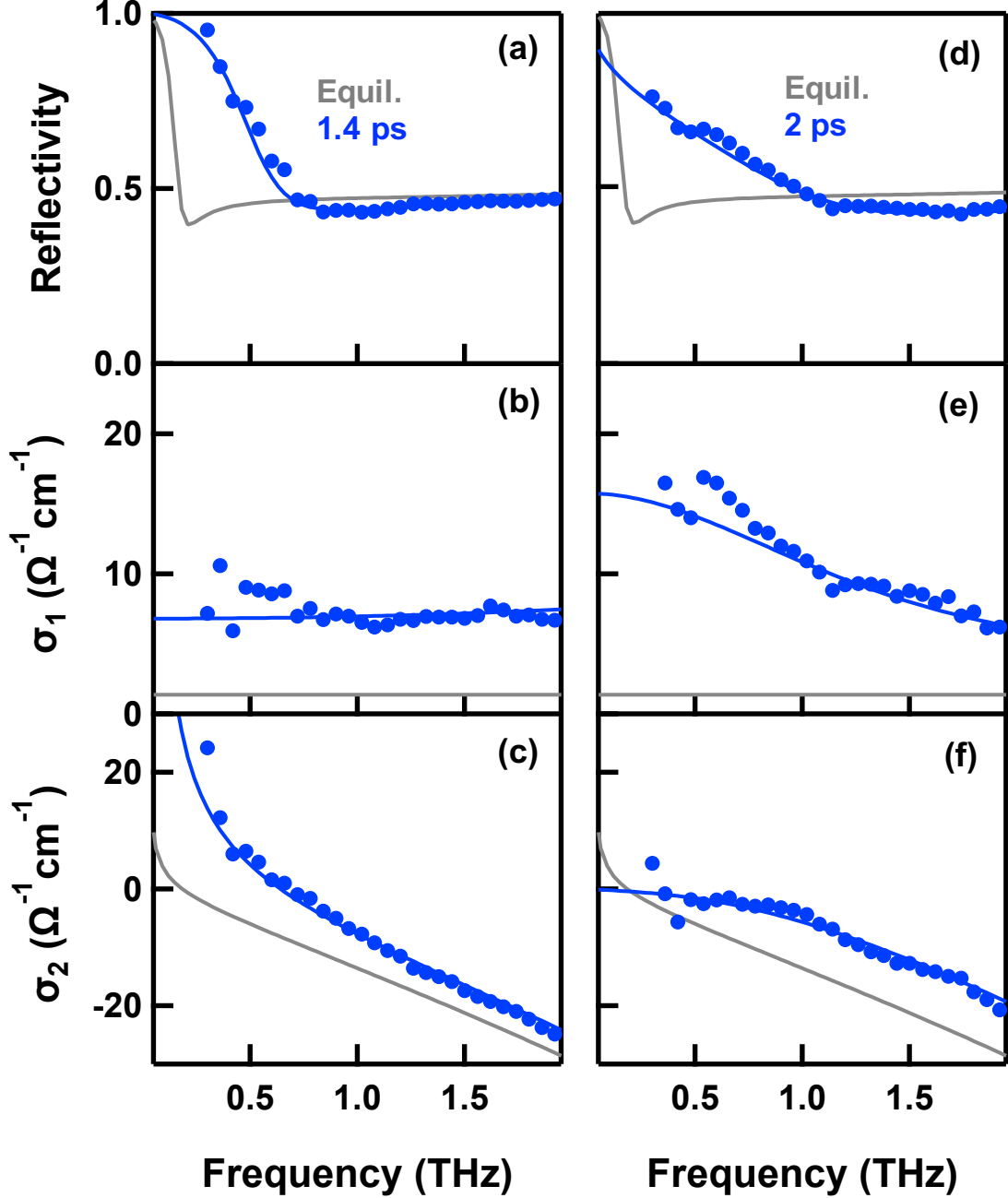


**Figure S1.** (a) *c*-axis THz reflectivity, (b) real, and (c) imaginary part of the optical conductivity of  $\text{La}_{1.885}\text{Ba}_{0.115}\text{CuO}_4$  measured at  $T = 5$  K (no magnetic field), at equilibrium (gray lines) and at  $\tau = 1.4$  ps pump-probe time delay (blue circles). Fits to the transient spectra are shown as blue lines. (d,e,f) Same quantities as in (a,b,c), measured at equilibrium (gray lines) and at  $\tau = 2$  ps time delay (blue). The transient data in (a,b,c) were fitted with a model describing the optical response of a Josephson plasma, while those in (d,e,f) with a Drude model for metals (see main text).

LBCO 11.5%  $T = 30$  K  $H = 0$

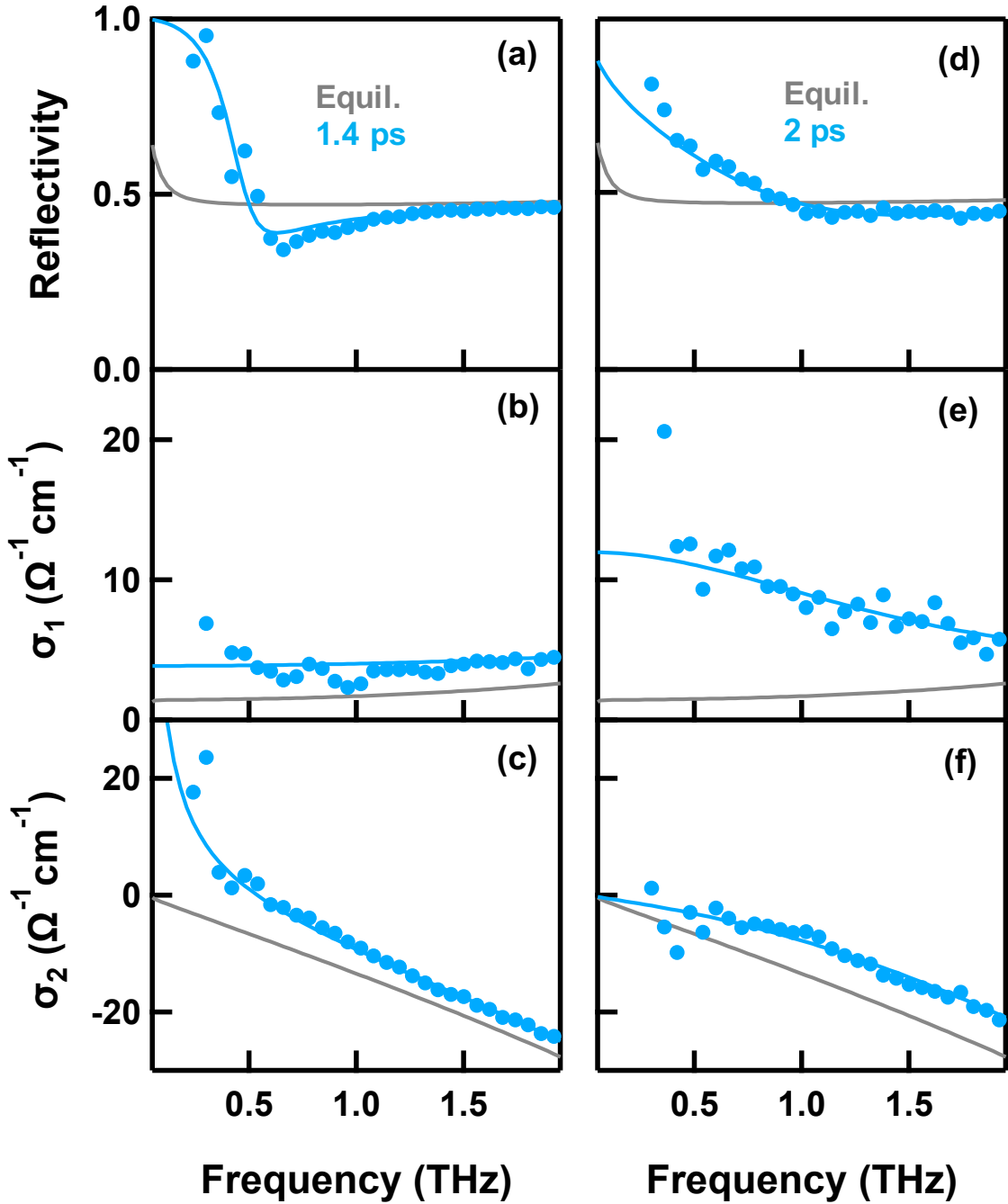


**Figure S2.** (a) *c*-axis THz reflectivity, (b) real, and (c) imaginary part of the optical conductivity of  $\text{La}_{1.885}\text{Ba}_{0.115}\text{CuO}_4$  measured at  $T = 30$  K (no magnetic field), at equilibrium (gray lines) and at  $\tau = 1.4$  ps pump-probe time delay (light blue circles). Fits to the transient spectra are shown as light blue lines. (d,e,f) Same quantities as in (a,b,c), measured at equilibrium (gray lines) and at  $\tau = 2$  ps time delay (light blue). The transient data in (a,b,c) were fitted with a model describing the optical response of a Josephson plasma, while those in (d,e,f) with a Drude model for metals (see main text).

LBCO 11.5%  $T = 5\text{ K}$   $H = 3.5\text{ T}$

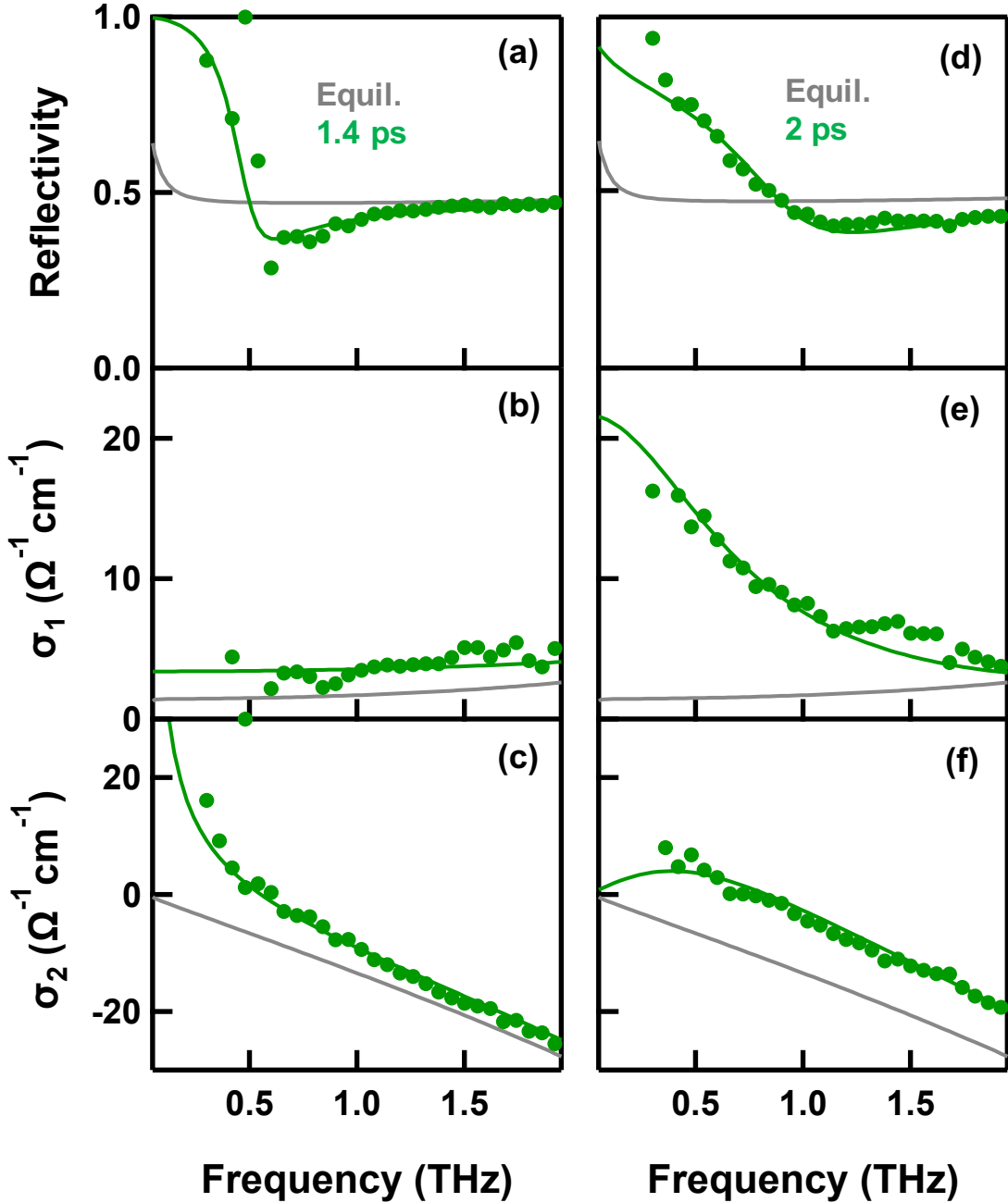


**Figure S3.** (a) *c*-axis THz reflectivity, (b) real, and (c) imaginary part of the optical conductivity of  $\text{La}_{1.885}\text{Ba}_{0.115}\text{CuO}_4$  measured at  $T = 5\text{ K}$  in a  $3.5\text{ T}$  magnetic field, at equilibrium (gray lines) and at  $\tau = 1.4\text{ ps}$  pump-probe time delay (green circles). Fits to the transient spectra are shown as green lines. (d,e,f) Same quantities as in (a,b,c), measured at equilibrium (gray lines) and at  $\tau = 2\text{ ps}$  time delay (green). The transient data in (a,b,c) were fitted with a model describing the optical response of a Josephson plasma, while those in (d,e,f) with a Drude model for metals (see main text).

LBCO 11.5%  $T = 5 \text{ K}$   $H = 7 \text{ T}$

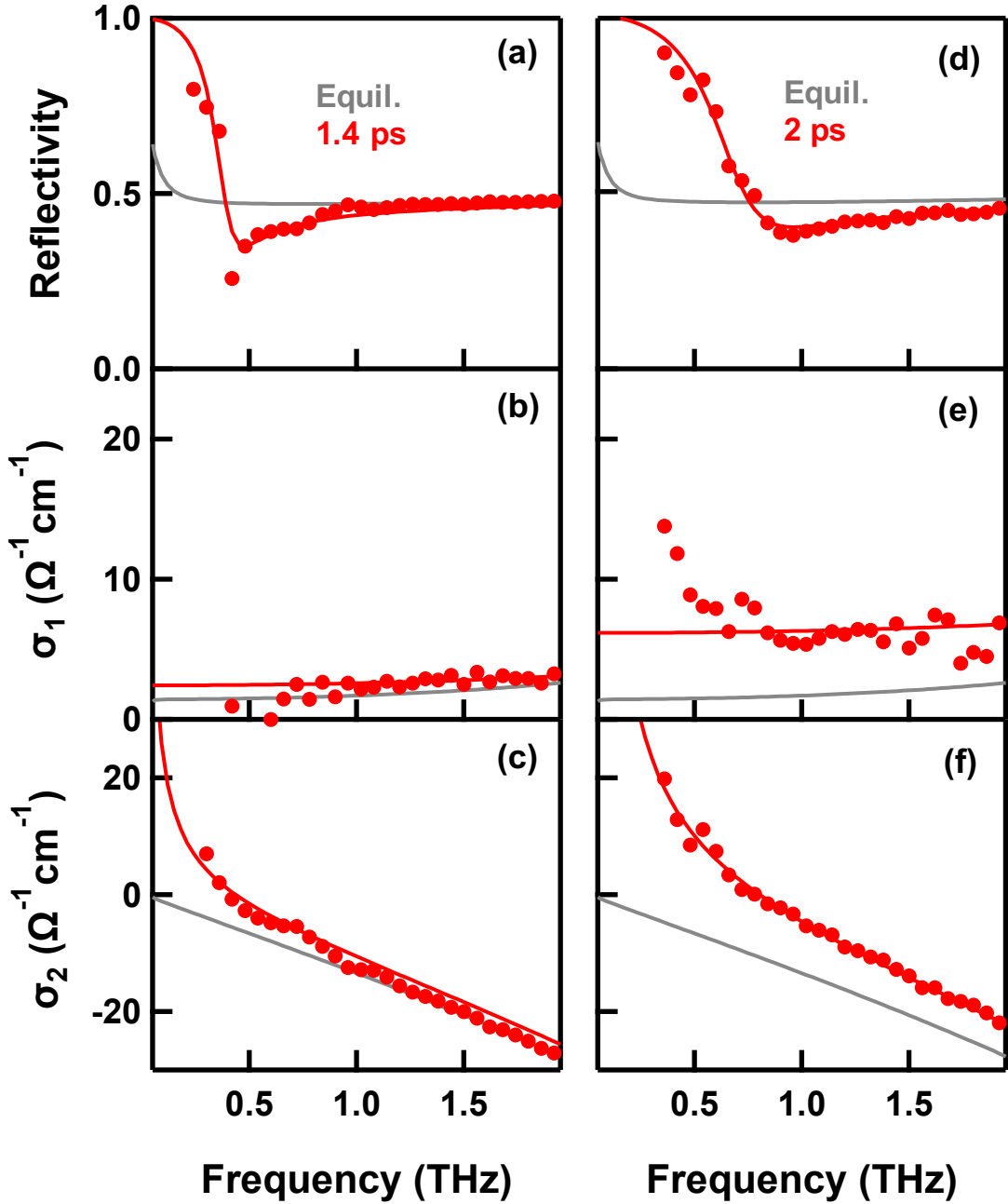


**Figure S4.** (a)  $c$ -axis THz reflectivity, (b) real, and (c) imaginary part of the optical conductivity of  $\text{La}_{1.885}\text{Ba}_{0.115}\text{CuO}_4$  measured at  $T = 5 \text{ K}$  in a  $7 \text{ T}$  magnetic field, at equilibrium (gray lines) and at  $\tau = 1.4 \text{ ps}$  pump-probe time delay (red circles). Fits to the transient spectra are shown as red lines. (d,e,f) Same quantities as in (a,b,c), measured at equilibrium (gray lines) and at  $\tau = 2 \text{ ps}$  time delay (red). All transient data were fitted with a model describing the optical response of a Josephson plasma (see main text).

LBCO 9.5%  $T = 5$  K

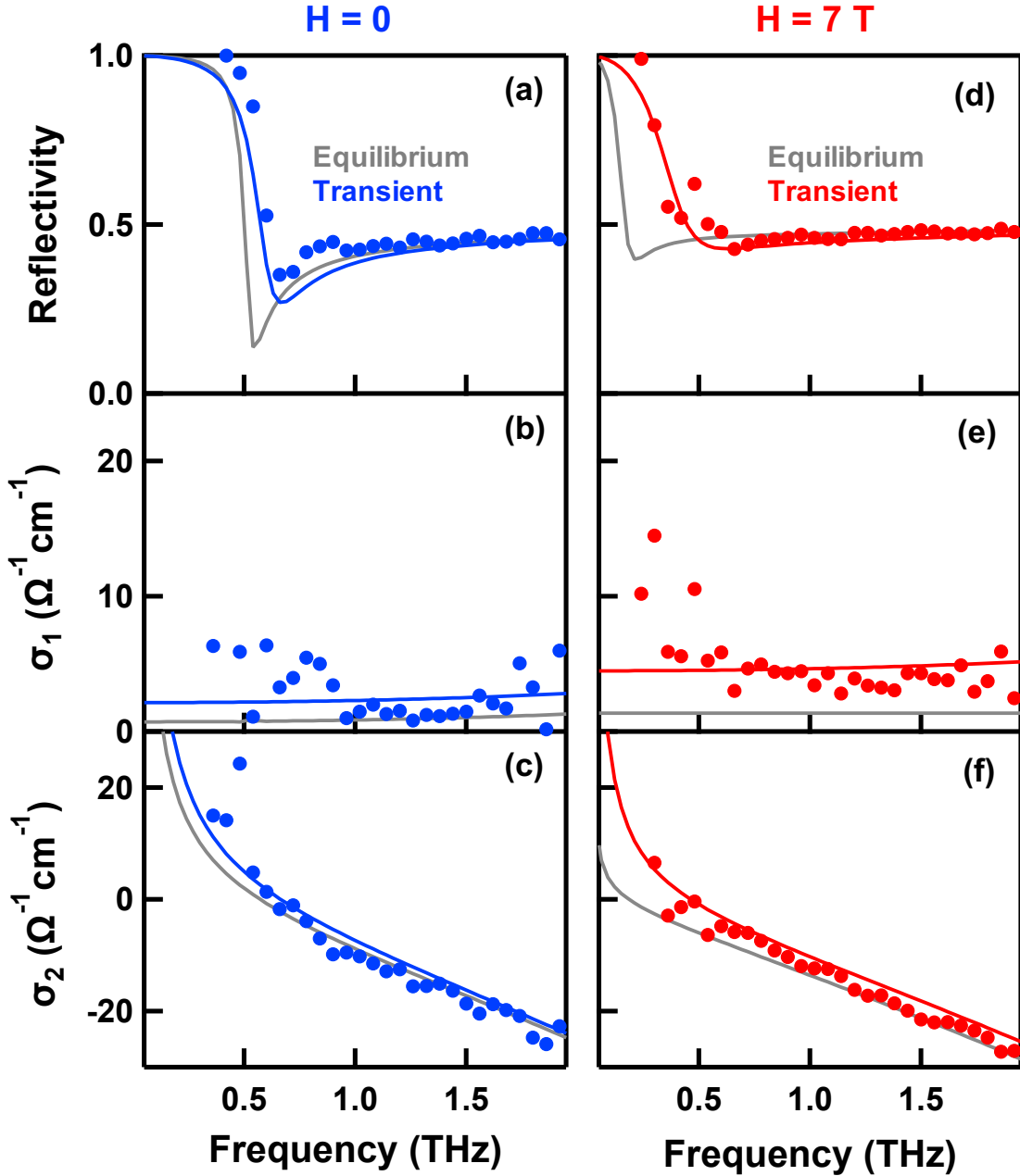


**Figure S5.** (a)  $c$ -axis THz reflectivity, (b) real, and (c) imaginary part of the optical conductivity of  $\text{La}_{1.905}\text{Ba}_{0.095}\text{CuO}_4$  measured at  $T = 5$  K (no magnetic field), at equilibrium (gray lines) and at  $\tau = 1$  ps pump-probe time delay (blue circles). Blue lines show fits to the transient spectra with a model describing the response of a Josephson plasma. (d,e,f) Same quantities as in (a,b,c), measured in  $\text{La}_{1.905}\text{Ba}_{0.095}\text{CuO}_4$  at  $T = 5$  K in presence of a 7 T magnetic field. Transient data, taken at  $\tau = 1.4$  ps, are shown here as red circles, while fits with the Josephson plasma model as red lines.